Critical Issues Concerning the Mechanisms of Duplex Grain Structure Formation and Interpretation of Duplex NiO Grown on Pure Ni and Cr Doped Substrates during High-Temperature Oxidation

C.K. Kim and L.W. Hobbs

Duplex layers are a very important class of film microstructures and form under a wide variety of conditions on a large number of substrates. In this paper, the available models for duplex layer formation are reviewed in detail and the basic assumptions which are based upon them are examined. The mechanisms of formation of the duplex layers based on microstructural observations in pure Ni and Ni-1at. % Cr systems during high-temperature oxidation are addressed.

Keywords
chromium, nickel, oxidation, theory

1. Introduction

THE GROWTH of an oxide film on a metal by thermal oxidation is usually discussed in terms of Wagner's theory, in which the oxidation rate is controlled by the transport of ions across the oxide film under the combined effects of concentration gradients and electric fields (Ref 1-4). This leads to parabolic growth kinetics with a single layer of oxide growth. However, in many cases, the oxide scales grown on the substrates at high temperature consist of two distinctive layers, an inner layer and an outer layer. These two layers have specific morphological characteristics. The inner layer consists of small equiaxed grains, while large columnar layers overgrow them.

There is considerable interest in the mechanism for formation of the duplex layer, since other important engineering systems, in addition to corrosion scales, exhibit a duplex layer, such as thin films deposited by sputtering or physical/chemical vapor deposition and solidified ingot microstructure. Therefore, it is worthwhile to review the available models for duplex layer formations, examine the basic assumptions which are based upon them, and compare them with other important engineering systems.

2. Critical Issues of the Models for the Duplex Growth

A number of models have been developed to explain why oxide scale grows in a duplex fashion.

2.1 *Dissociative Mechanism*

A dissociative mechanism was proposed by Mrowec to explain the compact outer portion and the porous inner portion of scales which are frequently found during optical microscopy or scanning electron microscopy (SEM) observation (Ref 5). As the oxidation reaction proceeds, growth stresses are generated within the oxide. In systems where cations are mobile, growth stresses arise in the scale, since the scale must relax to maintain contact with the metal. If the scale does not relax, voids will form at the scale/metal interface, separating the scale from the metal. Frequently this loss of contact causes the formation of a porous zone of scale between the outer compact layer and the metal. When scale separation occurs, the metal activity at the inner surface of the scale is high, and so cations continue to migrate outwards. However, this causes the metal activity to fall and the oxygen activity to rise correspondingly. As the oxygen activity arises, the oxygen partial pressure in local equilibrium with the scale inner surface rises, and oxygen evaporates into the pore, diffuses across the pore, and forms oxide on the metal surface (inner layer). In this way, a porous inner layer can be formed next to the oxide/metal interface while outward diffusion is maintained. The schematic of the dissociative mechanism is presented in Fig. 1.

The problem with this model is that the dissociation vapor pressure of the oxide is much too low to provide sufficient oxidant flux to account for the observed oxidation rates. It is also questionable whether the dissociative mechanism can be applied to the growth-protective chromia, alumina, or silica scales which exhibit duplex scales (Ref 6-9). The dissociative mechanism requires that scale growth occurs predominantly by cation diffusion, and it appears that this criterion is not met for

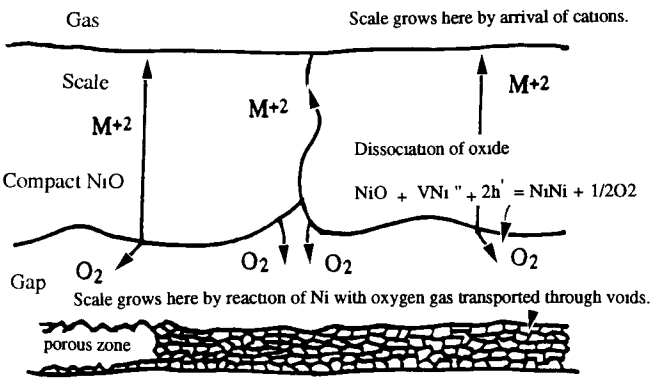

Fig. 1 Illustration of Mrowec's dissociative mechanism

C.K. Kim and **L.W. Hobbs,** Massachusetts Institute of Technology, Room 4-051, 77 Massachusetts Ave., Cambridge, MA 02139, USA.

alumina and silica, and perhaps not for chromia under certain conditions. Furthermore, if a void formed, for example at the interface between a chromia scale and its metallic substrate, the rate of transport of chromium vapor across the void could be greater than that of oxygen-bearing gases, thereby precluding the onset of pore formation by a dissociative mechanism.

2.2 *Lattice Diffusion of Cations and Grain Boundary Diffusion of Anions*

It is well established that the transport of cations and anions occurs along grain boundaries, since grain boundaries provide short circuit diffusion paths (Ref 10, 11). If the short circuit paths along grain boundaries are blocked by foreign atoms or precipitates, then the transport of ions will occur by lattice diffusion. Lattice diffusion of cations and grain boundary diffusion of anions can occur if the grain boundary segregants selectively occupy the cation sublattice sites along the grain boundary, resulting in the blockage of the cation short circuit diffusion paths. As far as the author is aware, this model is most likely among the available theories.

This model can be quantified on the modified parabolic rate law with the assumption that grain boundaries are the only effective short circuit diffusion paths. It is, therefore, useful to examine this model as one of the limiting cases of the model suggested by Smeltzer (Ref 12, 13).

As a limiting case, it may be assumed that f_t (the fraction of the cross sectional area of the oxide along which grain boundary diffusion can occur) is not a function of P_{O_2} and $D_O^b > D_{Me}^b$ and $D_{Me}^l > D_O^l$ where b is boundary, l is lattice, Me is metal, O is oxygen, and D is diffusivity. This case might be achieved if the segregation of foreign atoms blocks the available cation diffusion paths along grain boundaries. In this case, the parabolic rate constant (k_p) becomes:

$$k_p = k_p^l + \frac{1}{2} f_t \int_{P^i_{O_2}}^{P^a_{O_2}} D^l_{Me} \left(\frac{D^b_O}{D^l_{Me}} \right) d\ln P_{O_2} \qquad \text{(Eq 1)}$$

where P is pressure, a is ambient, and i is the metal/oxide interface.

It does not seem reasonable to assume that D_O^b/D_{Me}^l is independent of P_{O_2}. However, if D_O^b is independent of P_{O_2}, Eq 1 becomes:

$$k_p = k_p^l + \frac{f_t D^b_O}{2} \ln \frac{P^a_{O_2}}{P^i_{O_2}} \qquad \text{(Eq 2)}$$

To examine the relative contributions of lattice diffusion of cations and grain boundary diffusion of anions to the value of k_p, it is useful to replace k_p^l in Eq 2 with:

$$k_p^l = \frac{1+z}{\alpha} \frac{D^T_{Me}}{f_{Me}} \qquad \text{(Eq 3)}$$

where T is tracer diffusion.

Equation 3 is obtained when $P^a_{O_2} > P^i_{O_2}$, assuming that $Me_\alpha O$ is a p-type semiconducting compound (z is valence). Now we obtain:

$$k_p = \frac{1+z}{\alpha} D^l_{Me} + \frac{f_t D^b_O}{2} \ln \frac{P^a_{O_2}}{P^i_{O_2}} \qquad \text{(Eq 4)}$$

where D_{Me}^T is the tracer diffusion coefficient, f_{Me} is the correlation factor, and D_{Me}^T/f_{Me} has been replaced by the lattice self-diffusion coefficient for cations (D_{Me}^l). Typical values are $z = 2.0$, $\alpha = 1.0$, $f_t = 10^{-3}$ and $D_O^b/D_{Me}^l = 10^2$ to 10^5. If, for example, $D_{Me}^l = 10^{-12}$ cm^2/s, $D_O^b/D_{Me}^l = 10^2$, $P^a_{O_2} = 1$ atm and $P^i_{O_2} = 10^{-20}$ atm (values of 10^{-10} to 10^{-30} atm would be typical), then:[2]

$$k_p^l \text{ (lattice)} = f_t\, k_p^b \text{ (boundary)} \qquad \text{(Eq 5)}$$

In this case, transport of both anions and cations contributes significantly to scale growth, and new oxide may form within the existing layer.

2.3 *Oxygen Inward Transport*

Atkinson et al. performed tracer diffusion measurements on high-purity nickel and Ni-dilute Cr and Al alloys by sequential oxidation in O_2^{16} and O_2^{18} (Ref 14-20). In this experiment, the expected relationship between growth rate and diffusion constants was not confirmed and the oxidation rate was usually many orders of magnitude greater than expected. The investigators argued that for Ni oxidation, the fast rates are a result of rapid diffusion along grain boundaries in the oxide and that when this is taken into account, the oxidation rates and diffusion data can be reconciled. However, in the case of Ni-Cr and Ni-Al oxidation, even fast diffusion along grain boundaries is still apparently too slow to account for the measured oxide growth rates (Ref 21-26). Short circuit diffusion of oxygen appears to occur to a greater or lesser extent in practically all oxide films. Consequently, Atkinson et al. claimed that oxygen is transported as molecules along short circuit pathways and that this transport is responsible for the growth of new oxide within the films and for the growth of the inner layer of the well-developed duplex films which grow on the alloy. They proposed a

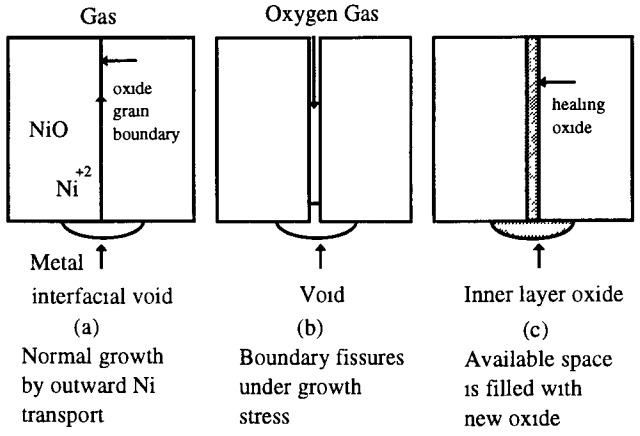

Fig. 2 Illustration of Atkinson's model for the inner layer

mechanism whereby oxygen gas penetrates the films through fissures to form new oxide in the available space. The actual pathways were not identified, but it is assumed that they are of a transient nature, i.e., they form, admit gas, then reseal during isothermal oxidation, as illustrated in Fig. 2.

Atkinson et al. suggested that duplex film formation is determined by the availability of space at the metal/oxide interface, i.e., the generation of interfacial porosity. The major questions which remain unanswered with this general explanation are how the fissures are generated in the growing field and how the porosity is generated at the metal/oxide interface.

2.4 *Available Space Model*

Almost the same idea is used in Manning's model (Ref 27), even though the oxygen pathways are different. The basis of this model is that single layers form when dislocation climb eliminates space created at this interface by outward metal diffusion. Factors which inhibit this volume collapse, such as sample corners or small quantities of certain impurities, lead to duplex scales. In these two models suggested by Atkinson and Manning, some porosity always exists in any growing scale, and a reaction at the oxide/metal interface directly initiates the inner duplex layer. These two models strongly depend on the movement of cation vacancies. According to them, vacancies will always arrive elsewhere at the oxide/metal interface and will pass into the highest metal plane. These vacancies will tend to condense into a series of vacancy-like dislocation loops (Fig. 3). It is less easy for the surrounding lattice to relax around these configurations, and their vacancy or microvoid character tends to be retained. Consequently, there is now space available for oxidation to occur at the interface if the oxidant has access to this interface as proposed. This process nucleates the inner layer. Oxidation proceeds until the space is filled with new oxide, which will form more inner layer oxide.

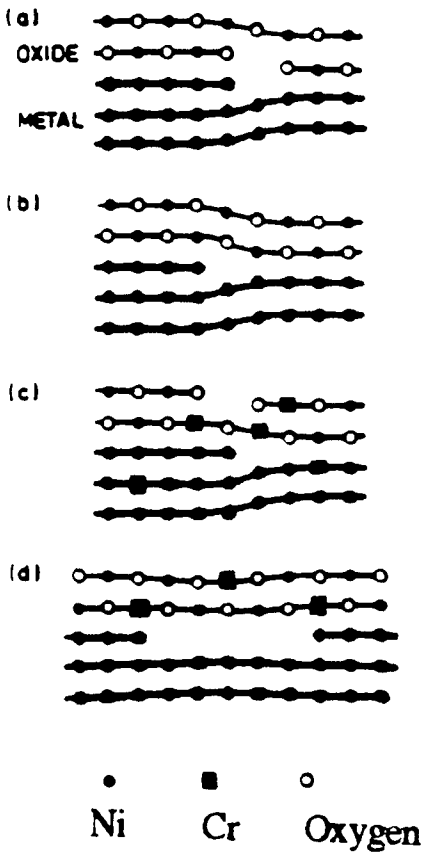

Fig. 3 Illustration of Manning's available space model. (a) Arrival of metal vacancy close to dislocation. (b) Climb of ledge by annihilation of vacancy. (c) Cr atoms can surround dislocation and prevent its climb. (d) Further arriving vacancies nucleate vacancy-like dislocation loop.

However, the fate of cation vacancies is still controversial (Ref 28-30). Several possibilities appear to be available to explain this vacancy flux: they accumulate at the interface as voids; they are annihilated at the interface by the climb of interface dislocations; or they diffuse into the metal, where they either form voids in the metal or are annihilated by the climb of metal dislocations.

2.5 *Gibbs and Hales' Mechanism (Revised Model of Mrowec's Dissociative Mechanism)*

Mrowec's dissociative mechanism has been revised by Gibbs and Hales (Ref 31). The Gibbs/Hales model has been considered an important reference model for duplex scale growth. It is a quasi-equilibrium model of duplex scale growth, analogous to Wagner's quasi-equilibrium model of single layer growth. It proposes that the oxidant can traverse the scale via pores which might form in the following manner. Metal diffusion along grain boundaries in the oxide creates an inward flux of vacancies. The vacancies could condense when they reach the oxide/metal interface and form cavities in the metal below the grain boundaries. A cavity would lower the oxidation rate locally and allow the oxide at the grain boundary to dissociate and open up into a pore (Fig. 4). Gas diffusion down the pore is rapid, and one pore of diameter 1 nm in the outer layer has been

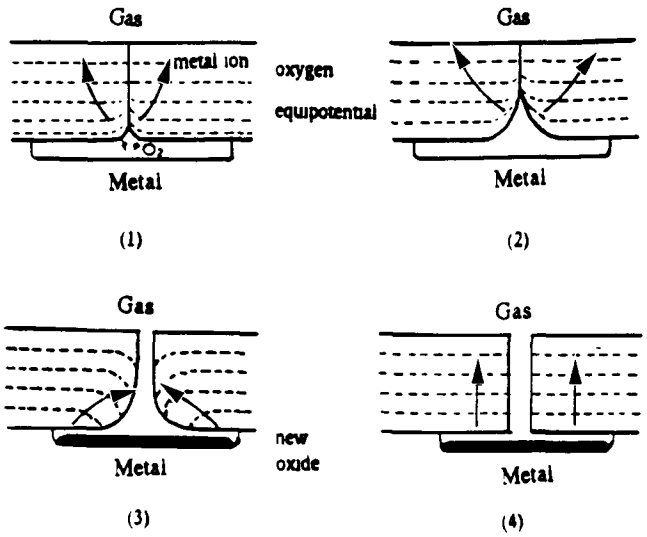

Fig. 4 Illustration of Gibbs and Hales mechanism. (1) Pore opens below oxide layer by vacancy condensation and dissociation of oxide. (2) Undersized pore grows by dissociation. (3) Oversized pore fills in by the reaction with metal ion. (4) Equilibrium-size pore remains since the oxygen activity near the pore is equal to that in the adjacent oxide.

found to provide sufficient access to account for the observed oxidation rates.

A question frequently raised about this model is why the pores do not simply block up. There appears to be nothing to prevent the outward-moving metal ions from meeting the inward-moving oxidant molecules, reacting in the pores, and filling them up. (This process was employed in the model of Rhines and Wolf, Ref 32). Gibbs and Hales argued that this need not happen if the equilibrium diameter varied across the scale in such a manner that the oxygen activity at any position in the pore was equal to that in the adjacent oxide. Pores of smaller diameter would open up by dissociation, while pores of larger diameter would attract a metal flux, which would tend to fill in the pore with a new oxide-forming inner layer.

However, it is questionable whether it is possible to apply concepts based on thermodynamics to a dynamic process such as the growth of scales. It has also been pointed out that pores tend to block, because the supply of oxidant is too large and so the oxygen activity along pore surfaces is too high (Ref 27).

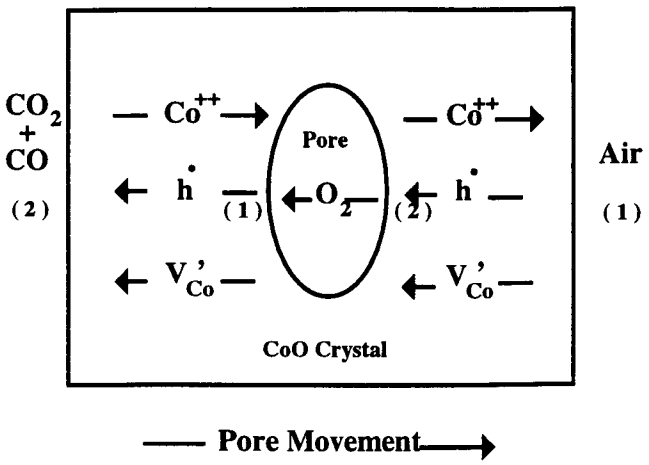

Fig. 5 Illustration of the pore movements in a cation-deficient oxide under oxygen potential gradient, suggested by Yurek and Schmalzried. P_{O_2} (1) > P_{O_2} (2). (1) $\frac{1}{2}O_2 + Co_{Co} + V'_{Co} + h + CoO$. (2) $V'_{Co} + h + CoO = \frac{1}{2}O_2 + Co_{Co}$.

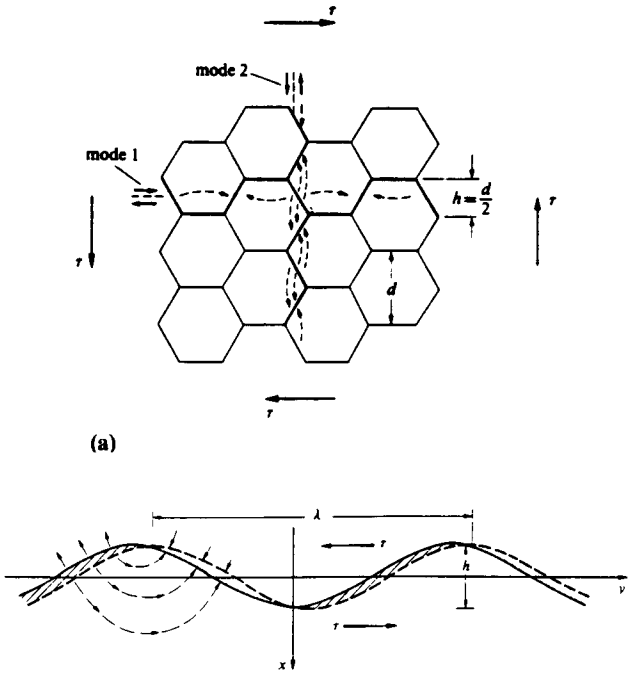

Fig. 6 Illustration of grain boundary sliding and the formation of a cavity. (a) Idealized model of a polycrystal as a hexagonal network of grain boundaries permitting grain boundary sliding according to two orthogonal modes. The accompanying vacancy flux is shown by the dotted arrows. (b) Sliding on a wavy grain boundary leads to the formation of a cavity (cross-hatched) which is transported as a vacancy flux into the overlap zones (dotted). Source: Ref 38

2.6 *Yurek and Schmalzried Mechanism*

This model is based on the same idea applied to the Mrowec and Gibbs-Hales models, i.e., the dissociation of the oxide. If an oxide single crystal is placed between two different oxygen potentials, the crystal begins to move toward the high potential side by diffusion of components (Ref 33, 34). Yurek and Schmalzried argued that in this way the total Gibbs energy of the overall system can be lowered. Experiments have shown that pores are formed in the originally nonporous single crystal at the lower-oxygen-potential interface and migrate to the higher-oxygen-potential interface (Fig. 5). Gas-filled pores are short circuit paths for the migrating vacancies.

It is therefore argued that this is the reason why smaller pores have a higher migration rate than bigger pores and why eventually smaller pores coalesce to form bigger ones. Pore formation of this kind has been found in single crystalline solid solutions as well as in stoichiometric compounds such as CoO or NiO. This model would require porosity to initiate at the metal/oxide interface and migrate through the scale. Estimates of pore migration rates in NiO from the fastest moving pores in CoO (0.15 cm/24 h) (Ref 34) yield values of 0.06 mm/h for pore migration in NiO. The estimate is based on the ratio of cation vacancy diffusivities D_V (NiO)/D_V (CoO) = 10^{-9} cm^2 s^{-1}/10^{-6} cm^2 s^{-1} = 10^{-3}, at 1200 °C used in each experiment. Therefore the application of this model to the NiO system seems unlikely.

2.7 *Evans' Model*

Evans et al. (Ref 35) suggested that the stresses produced by oxidation are a probable source of pores that serve as available space for inner layer growth. This porosity would be created either by the plastic deformation or the creep of the oxide. Evans et al. considered the plastic deformation of the rock salt structure oxide NiO growing on fcc Ni. In this system, the NiO grains are textured, being crystallographically oriented with respect to the substrate. According to the von Mises criterion, an arbitrary plastic deformation requires dislocation glide on five active, independent slip systems. In oxides, because of their ionic bonding, this is not likely to occur at typical oxidation temperatures, since only the primary slip systems such as {110}⟨110⟩ are likely to be active. Nevertheless, Evans et al. proposed that in the special case of NiO, because of texturing, the falling of the oxide toward the metal required for a single

layer could be accommodated by slip using only the primary slip systems. Presumably, in this model, alloying restricts this slip and so porosity builds up, leading to duplex growth. The problem with this mechanism is that it is specific to fcc metals, although the duplex layer formation is found generally in most oxidation systems.

2.8 *Kofstad's Model*

In any growing scale, the increase in volume accompanying oxidation creates a natural tendency toward compressive lateral stresses and longitudinal strains. Such strains cannot in general be accommodated in a polycrystalline oxide by dislocation glide, because too few slip systems are likely to be active at typical oxidation temperatures (Ref 36). This leaves creep as the remaining mechanism to relieve strain. Creep is the transport of matter in response to an applied stress and can involve intragranular diffusion, grain surface diffusion, and dislocation climb. When creep occurs in a polycrystalline oxide, it is likely to introduce porosity, as noted by Kofstad (Ref 37). Consider an array of hexagonal grains such as in Fig. 6. A vertical strain is produced by the flow of matter from the sides to the top and bottom of the grain. If this flow occurs without relative movement of the grains, voids are formed between the sides of the grains due to stresses (Fig. 7). This voiding can be relieved only by grain boundary sliding. The problem with this mechanism is that stress relief by diffusional creep or grain boundary sliding in the oxide is more difficult for scales with columnar microstructures than for fine equiaxed grains, because grain boundary sliding can hardly occur for a columnar microstructure.

2.9 *Recrystallization Model*

In this model, the outer layer of the oxide is explained simply as the evolution of initially formed inner layers by means of recrystallization. The driving force for recrystallization arises from the tendency to form larger oxide grains from grains which are either of smaller grain size or are more highly deformed than grains in the resultant recrystallized oxide. Since oxide scale morphologies generally manifest an increase in grain size with distance from the metal/oxide interface, this recrystallization model is a possibility.

2.10 *Duplex Layer Formation in Other Engineering Systems*

2.10.1 Duplex Layer Formation in Deposited Thin Films

The structure of as-deposited thin films is often discussed in terms of structure zone models such as those proposed by Movchan and Thornton et al. (Ref 39, 40). Thornton examined the microstructure of thick sputter-coated materials under a variety of temperature and pressure conditions. He concluded that the microstructures found were generally consistent with the three zone model proposed by Movchan and Demchishin. Three different zones were noted:

- At low argon pressures, a broad zone 1/zone 2 transition region consisting of densely packed fibrous grains was identified.
- Zone 2 columnar grains tended to be faceted at elevated temperatures, although facets were often replaced by smooth flat surfaces at higher temperatures.
- Zone 3 equiaxed grains were generally not observed at the deposition conditions investigated.

These modes all provide a general and highly qualitative picture of the expected film microstructure as a function of temperature. At low deposition temperatures, films generally exhibit an open columnar structure with extended voids along columnar grain boundaries. The columns themselves are not single grains but are composed of smaller, more equiaxed grains (inner layer). Increasing the film growth temperature results in a filling in of the voids, and a true columnar structure is obtained in which the columns are actually elongated grains. The boundary between these two structural zones is often stated to be at $T/T_m = 0.3$ where T_m is the melting point of the film.

While this provides a general guideline, it should not be taken literally. The transition between structural zones does not occur abruptly at any given temperature, i.e., it is not a structural phase transition. Moreover, an attempt to define a universal reduced transition temperature T/T_m ignores the strong dependence of nucleation and growth kinetics on critical parameters such as substrate structure and orientation, film growth rate, and the presence of impurities.

2.10.2 Duplex Grain Structure in Solidified Cast Material

When metal is solidified, the morphology of the grain structure is usually not uniform. The extent of the nonuniformity depends on the rate of cooling and other factors. When metal is poured into a metal mold, the metal in contact with the mold wall is cooled very rapidly. This high cooling rate at the surface influences the nucleation of crystals to a greater extent than their growth, with the result that many fine-grained equiaxed crystals are formed, as shown in Fig. 8.

With increasing thickness of the chilled zone of crystals, the temperature gradient from the liquid to the mold wall becomes less steep and the rate of cooling decreases. Crystal growth rather than nucleation of new crystals is then favored, and as a consequence the crystals at the liquid metal interface of the chilled zone begin to grow toward the center of the mold, forming long columnar crystals. Some crystals have orientations

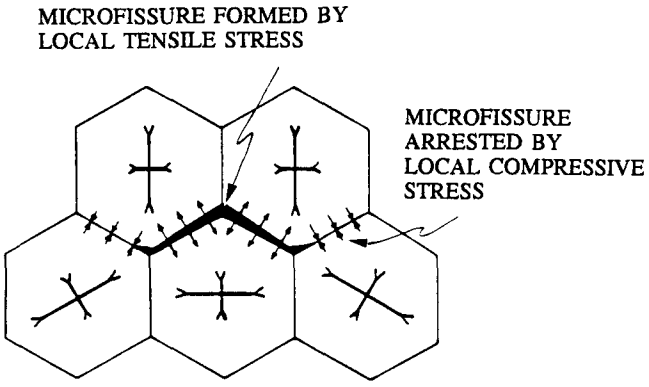

Fig. 7 Schematic drawing of the formation of microfissures due to localized tensile and compressive stress

such that their rapid growth direction, e.g., ⟨100⟩ in cubic crystals, is along the direction of heat flow, and hence they grow more rapidly than their neighbors. During growth, these crystals widen and stifle the growth of slower growing crystals from the chilled zone, so that this selective growth process gives rise to a preferred orientation in columnar grains.

In pure metals the columnar zone may extend to the center of the ingot, but in alloys, particularly, the liquid ahead of the growing columnar crystals is constitutionally undercooled and heterogeneous nucleation of new crystals takes place. These nuclei grow into coarse, randomly oriented, equiaxed crystals at the center of the ingot. A lowering of the temperature gradient increases the extent of the constitutional undercooling and hence the possibility of fresh nucleation. This is the condition that exists in the final stages of solidification in an ingot when the temperature gradients have largely flattened out.

3. Experiments

High-purity Ni (99.99%) and Cr (99.99%) were arc melted in an argon atmosphere to form a Ni-1at.% Cr alloy. After drop casting, the alloy underwent cold rolling to achieve 0.5 mm thickness. Strips of the pure Ni and Ni-1at.% Cr substrates which had $10 \times 25 \times 0.5$ mm geometry were cut from the resulting sheet. The substrate was mechanically polished sequentially from 600 grit SiC paper, 6 mm and 1 mm diamond paste down to 0.05 mm alumina powder. Samples were encapsulated in a vycor tube, evacuated to 1.5×10^{-4} Pa, and annealed in argon at 1123 K for several hours to achieve an average grain size of 200 μm.

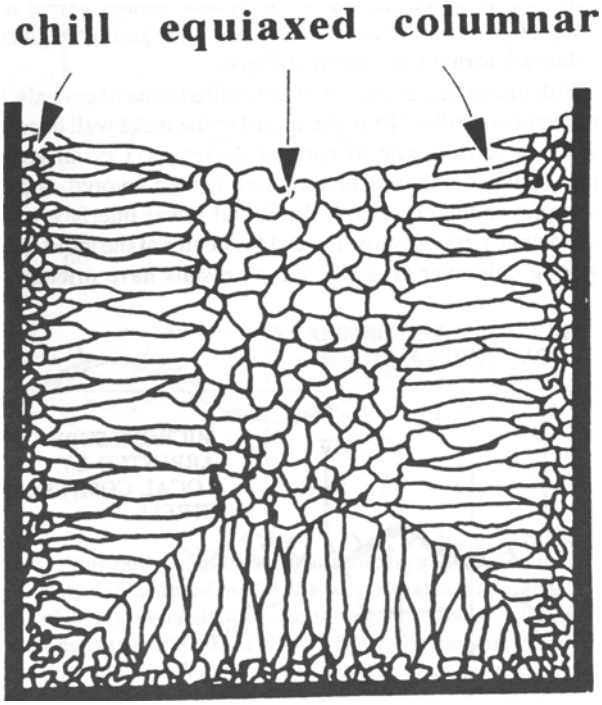

Fig. 8 Schematic drawing of a solidified cast structure showing the chill, columnar, and equiaxed zones

In order to identify diffusing species, a microlithographic marker experiment was designed. We have developed a technique for depositing inert markers of submicrometer dimensions onto metal substrates prior to oxidation (Ref 41, 42). The technique includes the microlithographic methods employed for semiconductor fabrication, involving generation of a pattern mask for exposing polymer resist through which sputtering of a marker material is made to form a pattern of line markers on the substrate.

Then, samples with and without markers were oxidized at 1273 K in air for various time durations and subsequently examined by SEM (Amray model 1000A and Cambridge model 250MK3), transmission electron microscopy (TEM) (JEOL model 200CX and Akashi model 002B), and scanning TEM (STEM, VG model HB501 with an energy dispersive x-ray windowless LINK LZ-5 detector). The ratio of the inner layer to outer layer of oxide with increasing oxidation time was determined with cross sectional TEM (XTEM) and SEM (XSEM) measurements.

4. Results

Various mechanisms proposed so far to explain the growth of the oxide layer during oxidation have not been based on actual microstructural observations. The microstructure and microchemistry through the oxide scale can be readily

Fig. 9 Transverse section image of TEM of a 5 min oxidation scale grown at 1273 K in air on the pure Ni substrate, showing the oxide layer composed of a single columnar layer

investigated by examination of transverse sections of oxide scales using TEM and SEM. Microstructural descriptions which are not presented in this paper can be found elsewhere (Ref 42-44).

For pure Ni, the oxide layer was composed of a single columnar type (Fig. 9) or inner layers of submicron thickness below a columnar layer (Fig. 10). Sometimes an intermediate layer with the smallest grain size was found between the columnar layer and the large inner layer (Fig. 11) (XTEM observation). Initial epitaxies between oxide and substrate were retained in the inner layer adjacent to the substrate. Epitaxial relationships determined by electron diffraction are given in Table 1.

Dilute addition of an alloying element (Cr) to the substrate significantly altered the oxidation mechanism as well as the microstructure (Ref 42-44) (marker experiment and XSEM and XTEM observations.)

For Ni-1at.%Cr, the oxide layer was composed of a thick inner layer with very small grain size and a columnar layer above (Fig. 12). The grains in the inner layers were randomly oriented. Initial epitaxially oriented grains were disturbed by formation of the inner layer (XTEM observation).

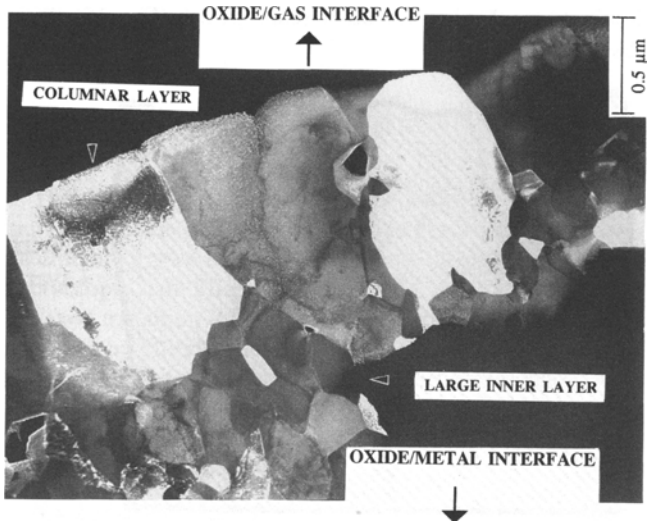

Fig. 10 Transverse section dark field image of a 15 min oxidation scale grown at 1273 K in air on the pure Ni substrate, showing the oxide layer composed of columnar layers overlying inner layer grains

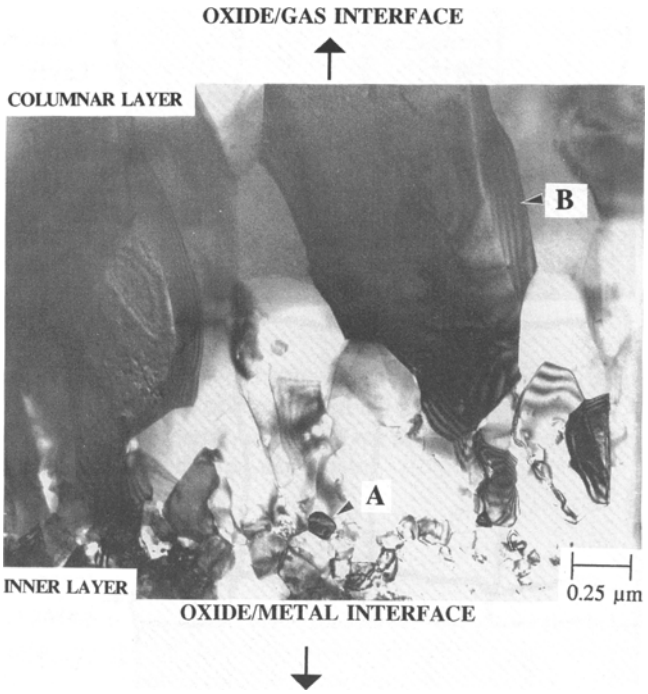

Fig. 12 TEM transverse section image of the oxide grown on the Ni-1at.%Cr substrate at 1273 K for 1 h, showing the large columnar layer growing above on the very small inner layer oxide grains

Table 1 Epitaxial relationship between inner layer of oxide grown on pure Ni and Ni substrate

(A)	$(001)\,[010]_{NiO}//(001)\,[010]_{Ni}$
(B)	$(111)\,[\bar{1}10]_{NiO}//(111)[1\bar{1}0]_{Ni}$
(C)	Four variants
	$(111)[01\bar{1}]_{NiO}//(001)[\bar{1}10]_{Ni}$
	$(111)[11\bar{2}]_{NiO}//(001)[\bar{1}10]_{Ni}$
	$(111)[10\bar{1}]_{NiO}//(001)[\bar{1}10]_{Ni}$
	$(111)[2\bar{1}\bar{1}]_{NiO}//(001)[\bar{1}10]_{Ni}$

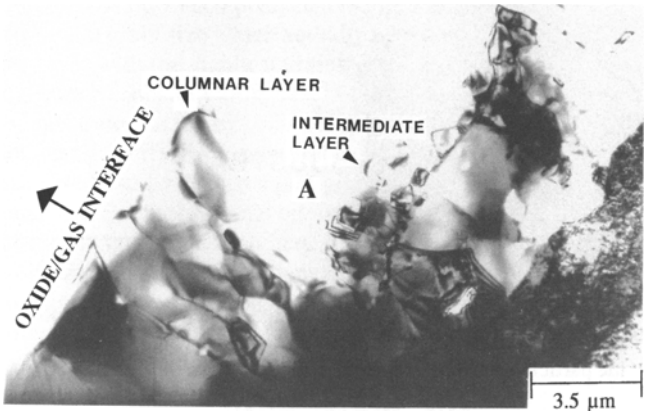

Fig. 11 Transverse section image of TEM of a 1 h oxidation scale grown at 1273 K in air on the pure Ni substrate, showing the intermediate layer (marked at A) between the inner and outer layer grains

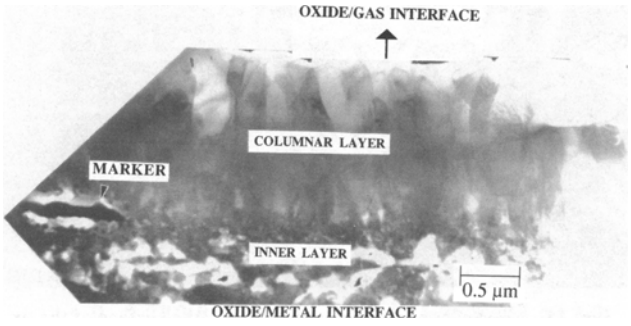

Fig. 13 XTEM bright-field image of NiO scale formed on Ni-1at.%Cr substrate oxidized 15 min at 1273 K in air, showing marker embedded in scale at the interface between the fine-grained inner layer and the largely columnar outer layer scales.

The markers were found to reside at the interface between a predominantly columnar outer NiO layer and a very fine-grained inner layer of NiO, indicating that the formation of inner layers is attributable to the oxygen inward transport (Fig. 13).

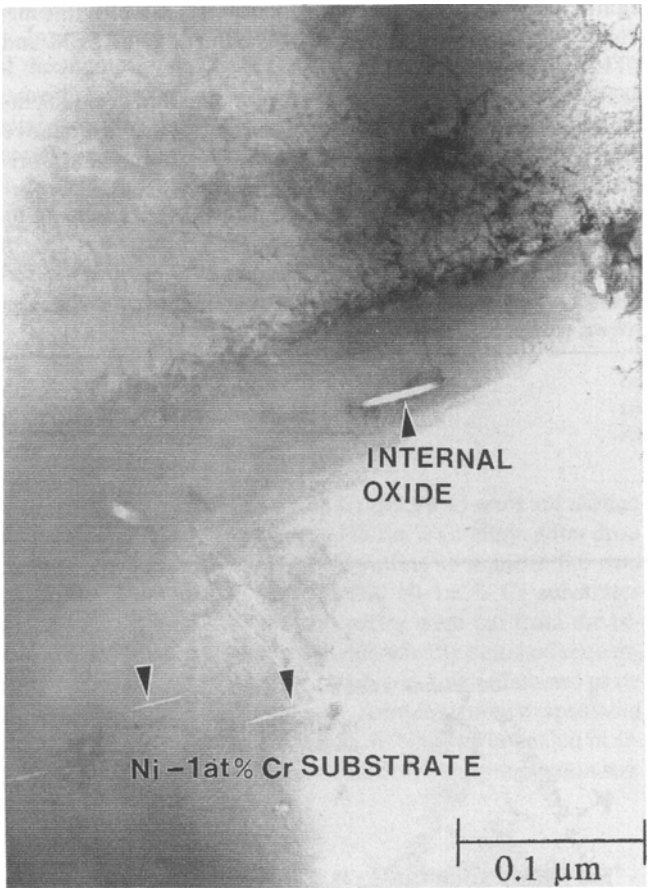

Fig. 14 TEM transverse section image of the Ni-1at.%Cr substrate after oxidation for 5 min at 1273 K, showing internal oxide particles just beneath the interface between oxide and metal

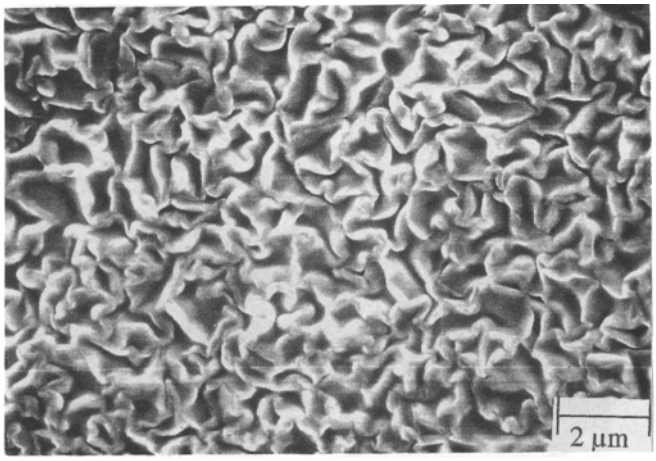

Fig. 15 SEM secondary electron image of the surface of the oxides formed on the Ni-1at.%Cr substrate at 1273 K for 2 h, showing ridges formed along emergent grain boundaries, indicating that the transport of the cation along the oxide grain boundaries is still the dominant transport mechanism.

At the shortest oxidation time used (5 min), oxygen ingress had occurred and formed Cr_2O_3 internal oxide particles in the Ni-Cr substrate. Numerous dislocations were observed at the metal/oxide interface (Fig. 14) (XTEM observation).

Grain boundary segregation of Cr was not detected at the outer layer columnar grain boundary for Ni-lat.%Cr at up to 1 h of oxidation, and the Cr was confined to the inner layer grain boundaries (Ref 21, 22) (STEM observation).

Ridges were found at the grain boundaries on the surface of the oxide for Ni-1at.%Cr after 2 h of oxidation, indicating that the transport of cations along the grain boundary is still the dominant mechanism for outer scale growth (Fig. 15) (SEM observation).

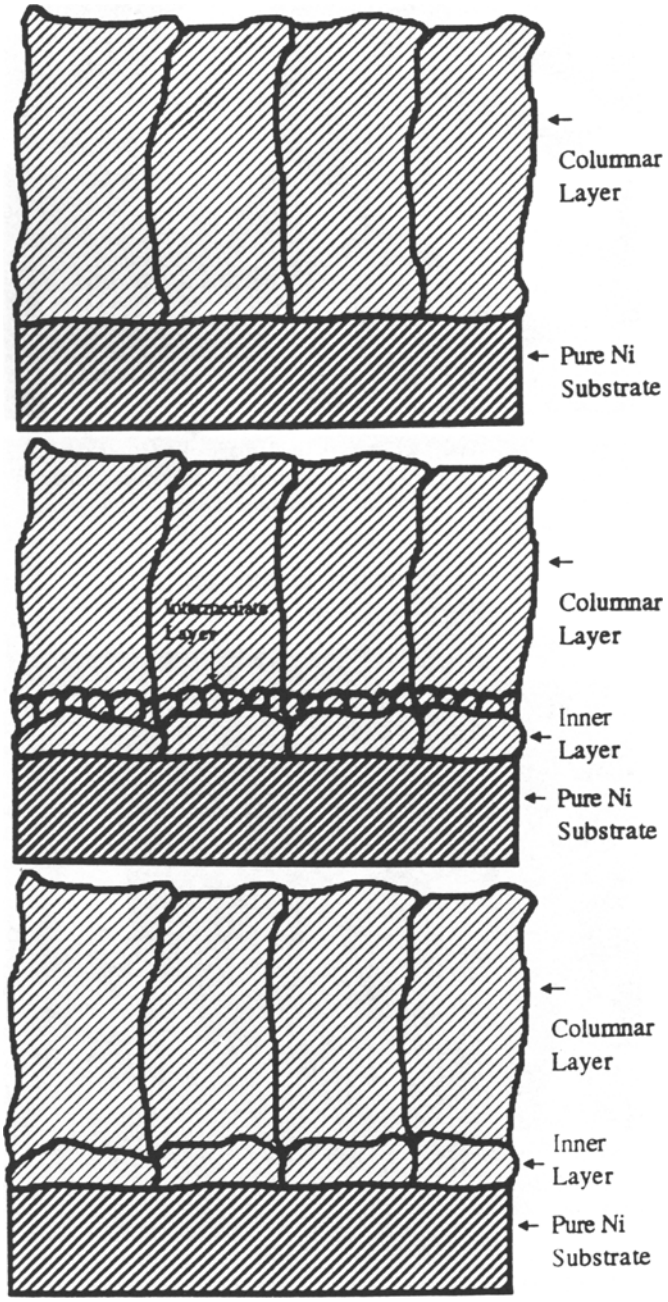

Fig. 16 Illustration of the three different oxide morphologies grown on the pure Ni substrate

For pure Ni, voids were observed to be distributed only within oxide grains after 2 h of oxidation, while for Ni-1at.% Cr, elongated pores formed extensively along the columnar oxide grain boundaries (Ref 43, 44) (TEM observation).

New fine-grained oxide formation in these pores was observed in case of the oxide grown on the Ni-1at.%Cr substrate after 2 h of oxidation (Ref 43, 44) (TEM and STEM observations). This new oxide sometimes completely resealed the void (Ref 43, 44) (TEM observation).

5. Discussion

5.1 *Proposed Growth Mode for the Oxide on Pure Ni Substrate*

The three modes of oxide growth found on pure Ni substrates are schematically represented in Fig. 16. The oxide microstructure grown on pure Ni substrate is very similar to the macroscopic solidified structure (Fig. 8). The columnar equiaxed transition found in solidified ingot structure can be explained by Tiller's analysis (Ref 45). In this theory, as x (distance ahead of a columnar dendritic interface) increases with time, the number of nuclei per unit volume N increases with x according to the relation given below:

$$N = Bx^2 \exp(-A/\Delta\mu^2) \quad \text{(Eq 6)}$$

where $\Delta\mu$ is the driving force for the reaction which is related to the constitutional supercooling, A is related to heterogeneous nucleation, and B is a constant. If the driving force increases with x, N would increase, giving a higher nucleation probability; consequently, equiaxed grains will appear.

A similar formalism can be derived on the basis of the nucleation and growth theory including oxidation parabolic rate kinetics, since the growth of an oxide on a substrate is one of the typical examples of the nucleation and growth phenomenon (Ref 46-52). The nucleation rate (I) is given as:

$$I = ND/a_0^2(-\Delta G^*/RT) \quad \text{(Eq 7)}$$

where N is the number of atoms/cm^3, D is diffusivity, a_0 is lattice parameter, and ΔG^* is the activation energy such that $\Delta G^* = 16\pi\gamma^3/3\Delta\mu^2$ (where γ is the surface energy). If spherical nuclei are assumed then we can obtain:

$$I \alpha \exp(-A/\Delta\mu^2) \quad \text{(Eq 8)}$$

where $\Delta\mu$ is the driving force and A is a complicated constant reflecting the influence of surface energy, temperature, and molecular volume of metal oxide. The growth rate (U) (Frenkel-Wilson growth or normal growth) is:

$$U = \lambda\nu = \lambda\nu_0 \exp(-\Delta G_a/RT)[1 - \exp(\nu\Delta\mu/RT)] \quad \text{(Eq 9)}$$

where λ is the distance between two phases, ν is the jump frequency across the phase boundary, and v is the volume of the transformed phase. For small driving force:

$$\cong \lambda\nu_0 \exp(-\Delta G_a/RT)(-v/RT)\Delta\mu \cong \text{constant } \Delta\mu \quad \text{(Eq 10)}$$

For parabolic oxidation kinetics:

$$\text{Growth rate} = k_p/x \quad \text{(Eq 11)}$$

where x is the oxide layer thickness. The characteristic grain diameter (D) is given as:

$$D = (U/I)^{1/4} \quad \text{(Eq 12)}$$

which leads to the following relationship between D and the distance from the oxide/metal interface (x):

$$D = A\,x^{-1/4} \exp(x^{1/2}) \quad \text{(Eq 13)}$$

A plot of Eq 13 is represented in Fig. 17. This plot shows the minimum grain size which actually appeared as the intermediate layer with the smallest grains in the oxide layer grown on the pure Ni substrate (Fig. 11). In the oxide growth on the pure Ni substrates, as in any solid-solid nucleation problem, the oxide/metal interfacial energy will be lower for the relative orientations of the two lattices that give good matching across the interface. For these special orientations, the nucleation rate will be much higher than for others. This particular orientation relationship between oxide and metal resulted in the epitaxial relationship (Table 1). Consequently, nuclei with only a few orientations were formed and grew rapidly along the favorable orientation, resulting in the columnar-type grains.

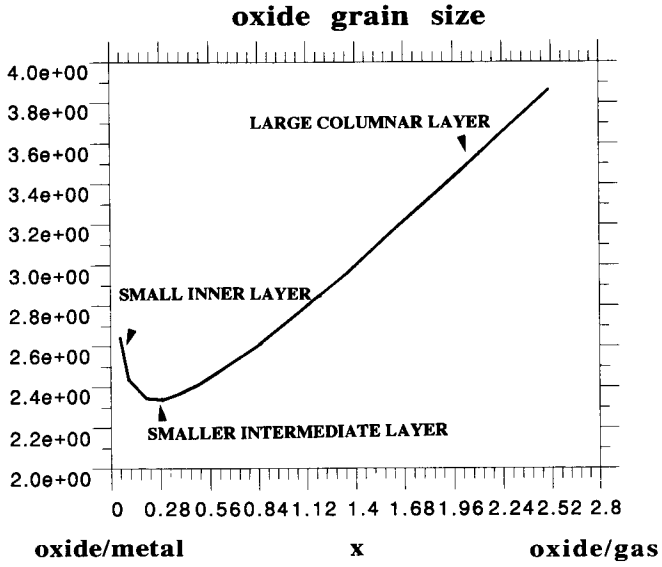

Fig. 17 Plot of the oxide grain size versus the distance from the oxide/metal interface

5.2 *Proposed Mechanism for the Oxide Grown on Ni-1at.% Cr*

5.2.1 Available Space for the Inner Layer Growth for the Oxide Grown on the Ni-1at.% Cr Substrate

The available models for the duplex layer formation presented in literature reviews have one common characteristic. All authors assume that specific microstructural features such as pores or voids, which will serve as the sites for new oxide growth, always exist in the oxide scale. It has long been argued by many researchers whether the dark holes in the inner layer observed using light microscopy or SEM represent porosity. Such pores and voids have not been observed in XTEM work, which indicates that the dark regions in the inner layer are artifactual small-grain pullout introduced during polishing. Consequently, models that assume available sites such as voids or pores for the inner layer growth are questionable. It is not necessary for any free volume (or available space) to be required if nucleation of new oxide occurs at other discontinuities such as dislocations (Fig. 14), and it is proposed that such defects provide the requisite nucleation sites for inner layer growth.

When two phases are situated such that the interface between them comprises a low index plane of each and within which at least one major crystallographic direction of each of the phases is parallel, the mismatch (or disregistry) between the phases can be expressed in terms of a mismatch parameter, δ. If the unit crystal dimension in the growing phase is a_0 and the equivalent dimension in the matrix is $a_0 + \Delta a$, the mismatch is given by $\delta = \Delta a/a_0$. If the lattice parameter of the growing phase and matrix is to match exactly, δ must be zero. On the other hand, if δ becomes too large (say $\delta > 0.25$), it is unrealistic to speak of any real registry between the phases, and the interface can be treated as an incoherent interface with other accommodation modes. When the value of δ is in the region of $\delta < 0.05$, the mismatch at the interface may be taken up by elastic strains in the lattices, and the boundary remains coherent. For intermediate values of δ, $0.05 < \delta < 0.25$, the elastic strain energy can be relieved by the formation of a network of dislocations in the interface, yielding a semicoherent boundary.

In the Ni/NiO system, δ is 0.19, necessarily resulting in accommodation dislocation densities in the interface. The most intriguing question about the oxide growth on Ni-1at.%Cr substrate is why oxygen ingress (which is evident from the marker experiment) to the substrate/oxide interface leads to formation of new inner layer oxide instead of growth of existing columnar grains. If new oxide at the oxide/metal interface due to oxygen ingress is formed heterogeneously on dislocations, it is not necessary for there to be any free volume (or available space), which is assumed in every proposed theory to be required. The heterogeneous nucleation of the new inner layer oxide at dislocations is consistent with the observed microstructures.

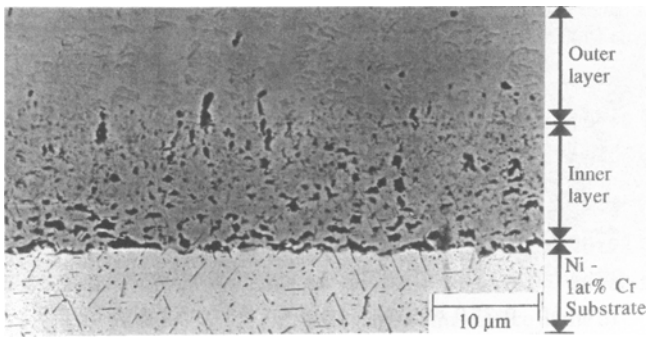

Fig. 18 SEM backscattered electron image of the oxide scale grown on Ni-1at.%Cr substrate at 1273 K, 5 h in air, showing the 1:1 inner and outer layer ratio

5.2.2 Oxygen Pathway for Inner Layer Growth

New oxide growth at the metal/oxide interface, observed in the marker experiment (Ref 42), requires the oxidant to be transported across the oxide layer. Since the measured diffusion rate of oxygen ions along grain boundaries and through the lattice is known to be much too slow to account for the observed microstructural growth (~1:1 ratio of inner and outer layers, Fig. 18), it is necessary to postulate that the oxidant has traversed the scale along some type of short circuit path (Ref 21-26).

Unambiguous observations of pipelike channels have not been reported from previous TEM studies. In general, postoxidation determination of the presence or absence of physical pathways cannot provide definitive evidence for behavior at the oxidation temperature. Nevertheless, it is proposed that when the inner layers of oxide form on the Ni-1at.%Cr substrate after long-time oxidation, the pathways of the oxygen are associated with the pores created due to the void coalescence along the grain boundaries. It should be noted that these observations are not artifactual results, since they were observed consistently over very large areas of specimens. Supporting microstructural evidences have been published elsewhere (Ref 42-44). Fore pure Ni, voids were observed to be distributed only within oxide grains. In contrast, for Ni-1at.% Cr, elongated pores formed extensively along oxide grain boundaries. Formation of new fine-grained oxide in these pores was observed to have sometimes completely resealed the voids. Other evidence is that grain boundary segregation of Cr was not detected at the outer columnar grain boundaries, which indicates that the cation transport along grain boundaries is still the dominant transport mechanism, so that formation of a duplex scale due to the blocking of the cation transport by the grain boundary segregation is not likely to have occurred. It can also be deduced, from the ridges formed along the grain boundaries on the surface of the oxides (Fig. 15), that a major transport mechanism by cation transport along grain boundaries is still operating. It is therefore proposed that the transport of oxygen for long oxidation times, in case of the oxide grown on Ni-1at.%Cr, occurs via pores formed by vacancy coalescence at the grain boundaries.

6. Conclusions

- NiO grown on the pure Ni substrate is wholly attributable to the outward cation diffusion. Three kinds of growth modes were observed. The oxide scales were composed of either a single columnar layer or a columnar layer overgrown on a thin inner layer. Sometimes an intermediate layer was observed between the columnar and inner layers. Initial epitaxies were retained in the form of inner layers. All of the

observed growth modes can be explained in terms of reduced nucleation rate toward the oxide/gas interface and growth along favorable orientations.

- NiO grown on the Ni-1at.%Cr substrate exhibited formation of a substantial inner layer with submicron grain size, established by the markers to have formed from oxygen ingress. Consequently, the initial epitaxies are disturbed by newly formed inner layer scale. The formation of a very fine-grained inner layer is ascribed to the heterogeneous nucleation of oxide at metal/oxide interface dislocations accommodating lattice disregistry.
- The suggested transport path of oxygen in the case of oxide scale grown on Ni-1at.%Cr substrate is voids (pores) formed by vacancy coalescence at the grain boundaries. These pathways are often found partially resealed by formation of new oxide within the voids along the grain boundaries.

Acknowledgment

Financial support from the National Science Foundation is gratefully acknowledged.

References

1. C. Wagner, *Prog. Solid-State Chem.*, Vol 10, 1975, p 3
2. C. Wagner, *Z. Phys. Chem.*, Vol B21, 1933, p 25
3. C. Wagner, in *Atom Movements*, American Society for Metals, 1951, p 153
4. C. Wagner, *Ber. Bunsenges. Phys. Chem.*, Vol 78, 1974, p 611
5. S. Mrowec, *Corros. Sci.*, Vol 7, 1967, p 563
6. C.M. Cotell, G.J. Yurek, R.J. Hussey, D.F. Mitchell, and M.J. Graham, *J. Electrochem. Soc.*, Vol 134, 1987, p 1871
7. C.M. Cotell, G.J. Yurek, R.J. Hussey, D.F. Mitchell, and M.J. Graham, *Oxid. Met.*, Vol 34, 1990, p 173
8. B.A. Pint, J.R. Martin, and L.W. Hobbs, *Oxid. Met.*, Vol 39, 1993, p 167
9. B.A. Pint and L.W. Hobbs, *Oxid. Met.*, Vol 41, 1994, p 203
10. A. Rahmel, G.C. Wood, P. Kofstad, and D.L. Douglass, *Oxid. Met.*, Vol 23, 1985, p 251
11. P. Kofstad, A. Rahmel, R.A. Rapp, and D.L. Douglass, *Oxid. Met.*, Vol 32, 1989, p 125
12. W.W. Smeltzer, R.R. Haering, and J.S. Kirkaldy, *Acta Met.*, Vol 9, 1961, p 880
13. J.M. Perrow, W.W. Smeltzer, and J.D. Embury, *Acta Met.*, Vol 16, 1968, p 1209
14. D.P. Moon, A.W. Harris, P.R. Chalker, and S. Mountfort, *Mater. Sci. Technol.*, Vol 4, 1988, p 1101
15. D.P. Moon, *Oxid. Met.*, Vol 31, 1989, p 71
16. A. Atkinson and D.W. Smart, *J. Electrochem. Soc.*, Vol 135, 1988, p 2886
17. A. Atkinson and R.I. Taylor, *J. Phys. Chem. Solids*, Vol 47, 1986, p 315
18. A. Atkinson and D.W. Smart, *High Temperature Materials Chemistry IV*, A. Munir, D. Cubicciotti, and H. Tagawa, Ed., The Electrochemical Society, 1987, p 296
19. A. Atkinson, *Mater. Sci. Technol.*, Vol 4, 1988, p 1046
20. D.P. Moon, *Oxid. Met.*, Vol 32, 1989, p 47
21. A. Atkinson, F.C.W. Pummery, and C. Monty, *Transport in Nonstoichiometric Compounds*, G. Simkovich and V.S. Stubican, Ed., Plenum, 1985, p 359
22. A. Atkinson, *Advances in Ceramics*, Vol 23, *Nonstoichiometric Compounds*, The American Ceramic Society, 1987, p 3
23. A. Atkinson, *Rev. Mod. Phys.*, Vol 57, 1985, p 437
24. A. Atkinson and A.E. Hughes, *Philos. Mag.*, Vol A43, 1981, p 1071
25. A. Atkinson, and R.I. Taylor, *Philos. Mag.*, Vol A39, 1979, p 581
26. A. Atkinson, R.I. Taylor, and P.D. Goode, *Oxid. Met.*, Vol 13, 1979, p 519
27. J. Robertson and M.I. Manning, *Mater. Sci. Technol.*, Vol 4, 1988, p 1064
28. R.E. Smallman and P.S. Dobson, *Surface and Defect Properties of Solids*, Vol 4, The Chemical Society, 1971, p 103
29. J.E. Harris, *Acta Met.*, Vol 26, 1978, p 1033
30. A.H. Heuer, "Vacancy Injection during Oxidation and Vacancy Injection during Oxidation—A Re-examination of the Evidence," Case Western Reserve University, 1977
31. G.B. Gibbs and R. Hales, *Corros. Sci.*, Vol 17, 1977, p 487
32. F.N. Rhines and J.S. Wolf, *Met. Trans.*, Vol 1, 1970, p 1701
33. G.J. Yurek and H. Schmalzried, *Ber. Bunsenges. Phys. Chem.*, Vol 79, 1975, p 255
34. G.J. Yurek and H. Schmalzried, *Ber. Bunsenges. Phys. Chem.*, Vol 78, 1974, p 1379
35. A.G. Evans, D. Rajdev, and D.L. Douglass, *Oxid. Met.*, Vol 4, 1972, p 151
36. J. Stringer, *Corros. Sci.*, Vol 10, 1970, p 513
37. P. Kofstad, *Oxid. Met.*, Vol 24, 1985, p 265
38. R. Raj and M.F. Ashby, *Trans. AIME*, Vol 2, 1971, p 1113
39. J.A. Thornton, *J. Vac. Sci. Technol.*, Vol 11, 1974, p 666
40. U. Helmersson, J.E. Sundgren, and J.E. Greene, *J. Vac. Sci. Technol.*, Vol A4, 1986, p 500
41. C.K. Kim, S.K. Fan, and L.W. Hobbs, *Microscopy of Oxidation*, G.J. Lorimer, Ed., Institute of Metals, London, 1991, p 374
42. C.K. Kim, *Oxid. Met.*, Vol 45, 1996, p 133
43. C.K. Kim and L.W. Hobbs, *Oxid. Met.*, Vol 45, 1996, p 247
44. C.K. Kim and L.W. Hobbs, Identification of Diffusing Species and Dynamic Nature of Diffusion Paths during Oxidation of a Dilute Ni-Cr Alloy, to be published in *Oxid Met.*, Vol 47 (No. 1/2), 1997, p 69-89
45. W.A. Tiller, *Physical Metallurgy*, R.W. Cahn, Ed., North Holland, Amsterdam, 1965
46. L.W. Hobbs, H.T. Sawhill, and M.T. Tinker, *Trans. Jpn. Inst. Metals*, Vol 3, Suppl., 1983, p 115
47. L.W. Hobbs, H.T. Sawhill, and M.T. Tinker, *Rad. Effects*, Vol 74, 1983, p 229
48. H.T. Sawhill, L.W. Hobbs, and M.T. Tinker, *Adv. Ceram.*, Vol 6, 1983, p 128
49. H.T. Sawhill and L.W. Hobbs, *Proc. Int. Congr. on Metallic Corrosion*, Vol 1, 1984, p 21
50. M.T. Tinker and P.A. Labun, *Oxid. Met.*, Vol 18, 1982, p 27
51. M.T. Tinker, Ph.D. thesis, Case Western Reserve University, 1984
52. H. Sawhill, Ph.D. thesis, MIT, 1985